

Temperature modulation of the optical transitions involving the Fermi surface in Ag: Experimental

R. Rosei

Istituto di Fisica, Università di Roma, Roma, Italy
and Gruppo Nazionale di Struttura della Materia of the Consiglio Nazionale delle Ricerche, Roma, Italy

C. H. Culp* and J. H. Weaver†

Ames Laboratory-USAEC and Department of Physics, Iowa State University, Ames, Iowa 50010

(Received 16 August 1973)

Thermoreflection and thermotransmission measurements were made on thin semitransparent films of Ag at about 320, 120, and 15 K in the range 3.40–4.40 eV. The results are in fairly good agreement with the theory presented in the preceding paper but show that thin metal films evaporated on amorphous substrates become strained upon cooling to low temperature. The onset of the $L_3 - L_2'(E_F)$ transition is found to be at 4.03 eV, while the onset of the $L_2'(E_F) - L_1$ transition occurs at 3.87 eV.

I. INTRODUCTION

The technique by which the static and thermode-
rivative imaginary part of the dielectric constant
can be calculated for interband transitions involving
the Fermi surface in noble metals was discussed
in the preceding paper,¹ with special reference to
Ag. Part of the theoretical results have been ex-
perimentally verified by low-temperature thermo-
modulation measurements on Au.² Ag should pro-
vide an almost ideal check: Interband transitions
occur, in fact, in a spectral region where the in-
traband contribution to the absorption has almost
vanished, clearing the spectra of any unwanted
Drude background. Besides, it is known that both
 d -band-to-Fermi-surface transitions and inter-
conduction-band transitions contribute to the steep
absorption edge at about 3.9 eV. Therefore the
calculated behavior of both kinds of transition can,
in principle, be checked.

The comparison of low-temperature thermode-
rivative data on Ag with the theory also may pro-
vide a useful assessment of the whole situation
which has received particular attention in the last
few years.³⁻⁷ Baldini and Nobile⁸ have measured
the thermoderivative response of Ag at room tem-
perature (RT) and, assuming that their film was
opaque, performed a Kramers-Kronig analysis of
their fractional-reflectivity data in order to obtain
the spectrum of $\Delta\epsilon_2$. Their results agree fairly
well in over-all shape with the theory presented in
the preceding paper.¹ Unfortunately, volume mod-
ulation and the modulation of the broadening param-
eter are not negligible at room temperature,⁹ and
thus the expected response of the weaker $L_2'(E_F)$
 $- L_1$ transitions may remain hidden in the strong
thermoderivative signal arising from the $L_3 - L_2'(E_F)$
transitions. Also, the procedure of Kramers-
Kronig-analyzing data of fractional reflectivity
 $\Delta R/R$ for a film not completely opaque may lead to

errors in the calculated spectrum of $\Delta\epsilon_2$. In the
following we present thermoderivative spectra of
Ag taken near RT, liquid-nitrogen temperature
(LNT), and liquid-helium temperature (LHeT).
Both the fractional change of the reflectivity, $\Delta R/R$,
and the transmission, $\Delta T/T$, have been measured.
The comparison of the experimental results with
the theory allows the determination of several band
gaps and the evaluation of the contribution of the
two different transitions to the total absorption.

II. EXPERIMENTAL

The basic experimental technique has been de-
scribed in a previous paper.⁹ The Ag samples
were prepared in a vacuum of 10^{-7} Torr during
evaporation. Ag was evaporated from a tungsten
boat onto a flat fused-quartz substrate, $25 \times 25 \times 5$
mm. The film was measured to be 520 Å thick with
a Varian multiple-beam interferometer. Errors
in the thickness measurement were about 10% with
this technique. The sample was clamped to a cold
finger in a cryostat immediately after removal
from the evaporator, and a vacuum of 10^{-6} Torr
was reached in this cryostat within 30 min.

A Perkin-Elmer 99 prism double-pass mono-
chromator gave double- and single-pass light from
a xenon arc lamp. Since the internal chopper was
not used, a Bausch and Lomb grating monochroma-
tor was used to filter out the single-pass light from
the prism monochromator. An EMI 6256B photo-
multiplier detected the energy range required,
from 3.4 to 4.4 eV. A 7-Hz square wave from a
power amplifier provided the temperature modula-
tion for the Ag. Typically, 0.15 to 1.5 W of peak
power were dissipated in the sample. Data were
taken in a point-by-point manner with the I_0 or light
level held constant. The dc voltage on the photo-
multiplier load resistor was read with a digital vol-
tmeter. The small ac voltage was read using a
Keithley phase-sensitive amplifier, the output of

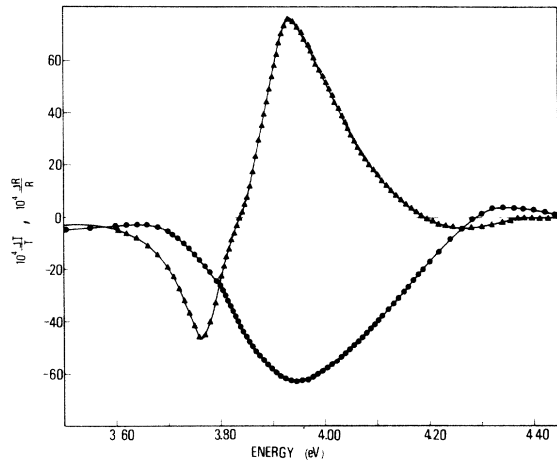


FIG. 1. Thermotransmission and thermoreflexion spectra of a 520-Å-thick film of Ag at 320 K. Peak power 0.8 W. Line through circles, $\Delta T/T$; line through triangles, $\Delta R/R$.

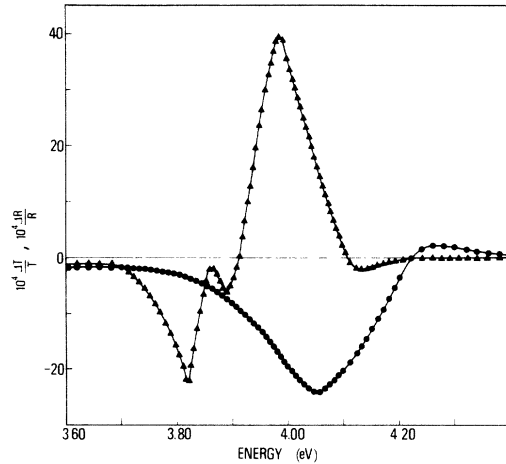


FIG. 3. Thermotransmission and thermoreflexion spectra of a 520-Å-thick film of Ag at 15 K. Peak power 0.15 W. Line through circles, $\Delta T/T$; line through triangles, $\Delta R/R$.

which went to a voltage-to-frequency converter and then to a counter for integration, typically for 100 sec.

The minimum detectable signal for $\Delta R/R$ or $\Delta T/T$ was about 5×10^{-6} . Most of the data were of the order of 10^{-4} or larger, with a reproducibility of better than 5%.

III. RESULTS AND DISCUSSION

The experimental spectra of the fractional change in film reflectivity, $\Delta R/R$, and the fractional change in film transmissivity, $\Delta T/T$, obtained with a 520-Å film of Ag near RT, LNT, and LHeT are shown in Figs. 1-3. The spectrum of $\Delta R/R$ at RT (Fig. 1) shows the well known derivative structure⁸

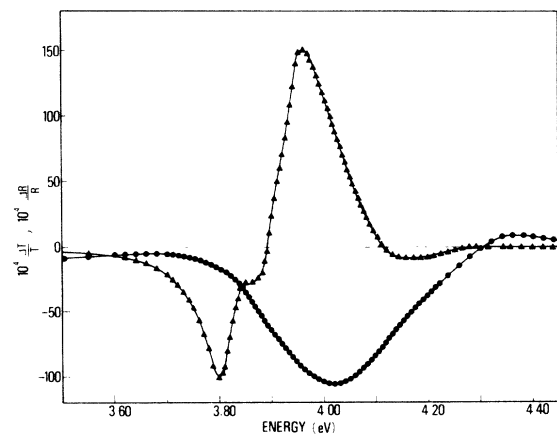


FIG. 2. Thermotransmission and thermoreflexion spectra of a 520-Å-thick film of Ag at 120 K. Peak power 1.4 W. Line through circles, $\Delta T/T$; line through triangles, $\Delta R/R$.

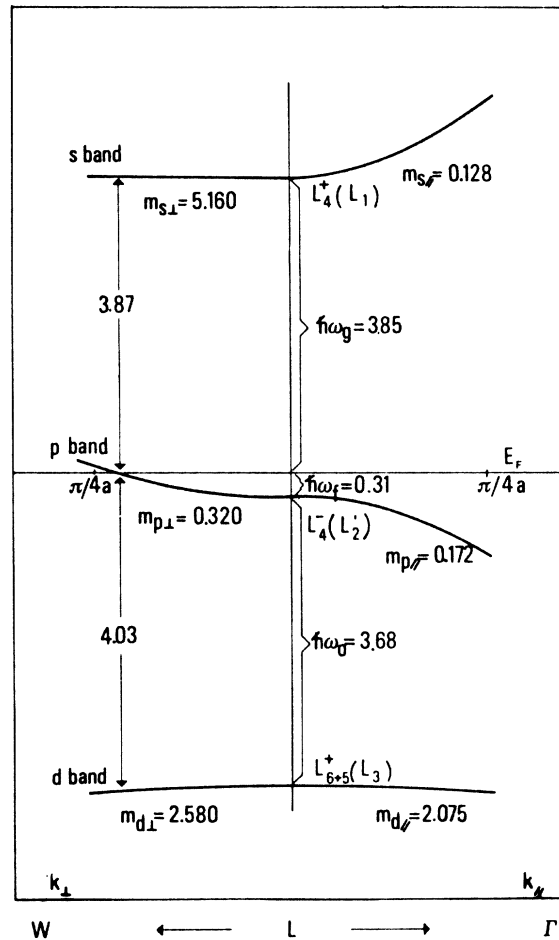


FIG. 4. Detail of band structure near L for Ag. The effective masses were calculated from Ref. 6 and the gap values from the fitting of experimental data.

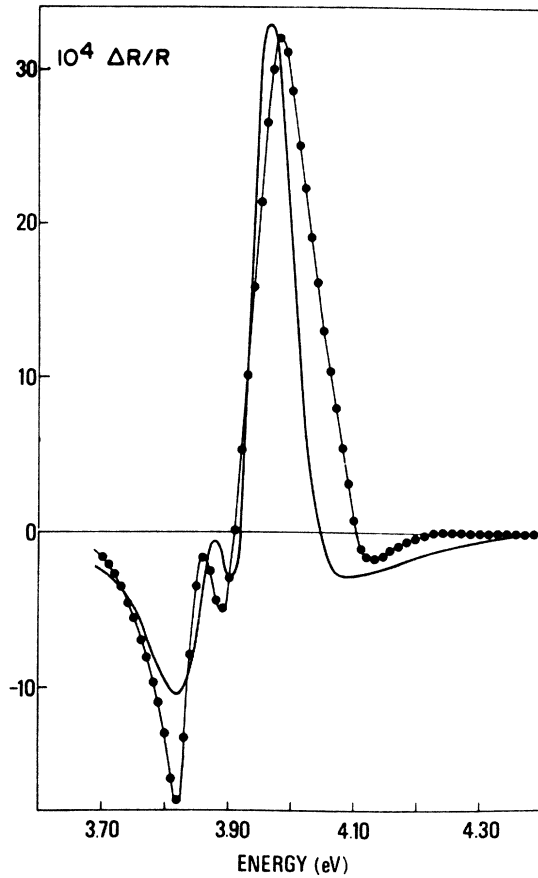


FIG. 5. Thermoreflection spectra of Ag. Line through circles, experimental (~ 15 K); solid line, theoretical.

and a slight shoulder at about 3.82 eV which has not previously been observed. On lowering the temperature, the derivative structure sharpens and moves to higher energies. The shoulder in $\Delta R/R$ becomes more pronounced and moves to 3.86 eV at LNT. Close to LHeT (~ 15 K) the shoulder has become a separate peak, and the derivative structure has sharpened further, but not as much as one might expect on a theoretical basis.¹

The spectra of $\Delta T/T$ are much simpler and seem to indicate that the main effect is a decrease of transmission with increasing temperature. It is somewhat surprising, however, not to find structures at about 3.86 eV in correspondence to the structure in $\Delta R/R$.

In order to interpret the data and have a direct comparison with theoretical calculations, we have attempted to calculate $\Delta\epsilon_1$ and $\Delta\epsilon_2$ from the spectra of $\Delta R/R$ and $\Delta T/T$.¹⁰ This proved to be difficult for Ag, since the calculated $\Delta\epsilon_1$ and $\Delta\epsilon_2$ show very large, sharp spurious structures. It was found that these were an artifact of the method of inversion of the formulas for thin films. It should be mentioned that similar difficulties have been en-

countered by several authors when attempting to get ϵ_1 and ϵ_2 data from static R and T measurements on Ag thin films.¹¹⁻¹³

To avoid these difficulties, the theoretical line shape of $\Delta\epsilon_2$ has been used to calculate the expected $\Delta R/R$ and $\Delta T/T$. The theoretical $\Delta\epsilon_1$ was calculated via Kramers-Kronig analysis of $\Delta\epsilon_2$; $\Delta\epsilon_1$ and $\Delta\epsilon_2$ data were then inserted in formulas for thin films¹⁴ to yield the spectra of $\Delta R/R$ and $\Delta T/T$.¹⁵

To obtain agreement with the experimental structures, it was decided to use as free parameters the positions of the points L_3 , L'_2 , and L_1 with respect to the Fermi surface and the relative magnitude of the oscillator strength of the $L_3 \rightarrow L'_2(E_F)$ transition and the $L'_2(E_F) \rightarrow L_1$ transition. As an additional constraint, we required that the theoretical ϵ_2 obtained with these parameters should fit ϵ_2 experimental data (taken from Ref. 11).

The effective masses were obtained from Christensen's relativistic augmented-plane-wave (RAPW) band-structure calculation⁶ by fitting parabolas through his calculated points, with the exception of $m_{p,1}$, which was determined using the experimental neck radius¹⁶ of the Fermi surface and the value of

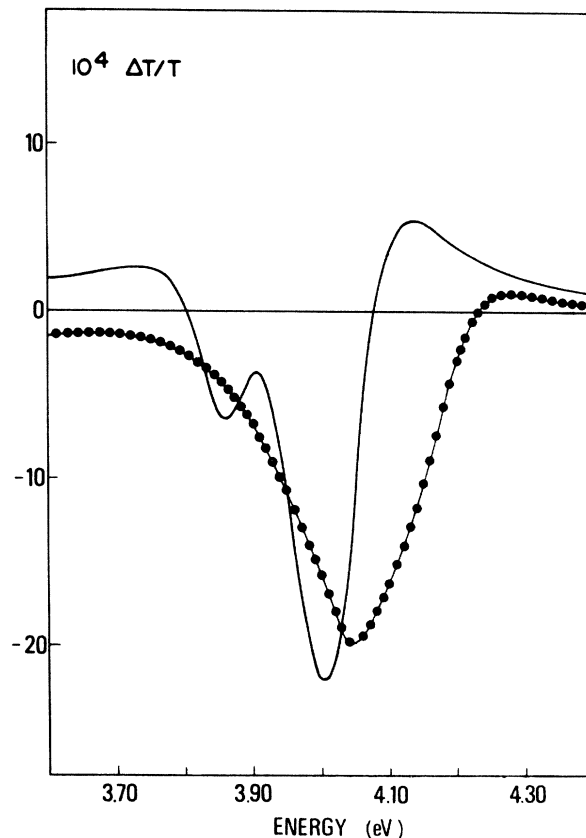


FIG. 6. Thermotransmission spectra of Ag. Line through circles, experimental (~ 15 K); solid line, theoretical.

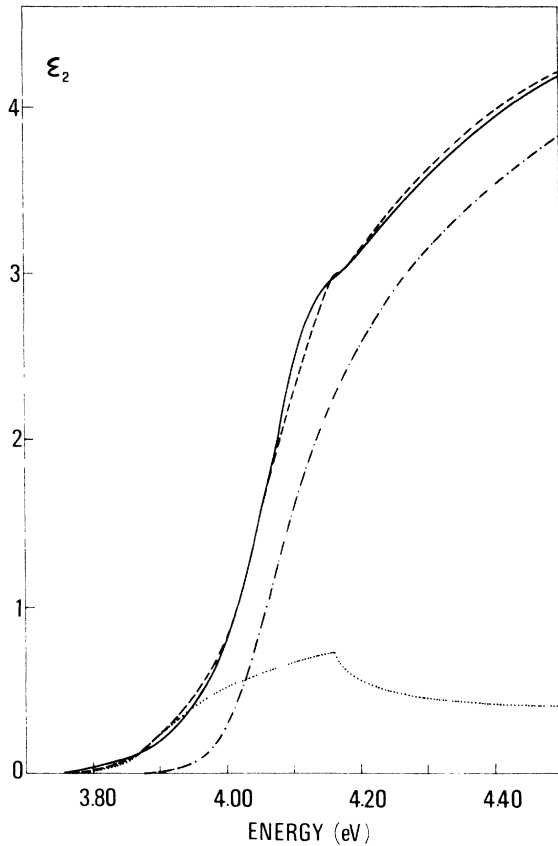


FIG. 7. Imaginary part of the dielectric constant for Ag: solid line, experimental (from Ref. 11); dotted line, calculated $L_2'(E_F) \rightarrow L_1$ contribution; dot-dashed lines, calculated $L_3 \rightarrow L_2'(E_F)$ contribution; dashed line, total theoretical.

the $E_F \rightarrow L_2'$ energy separation.¹⁷ The parameters used for the theoretical computation are reported in Fig. 4.

Only the lowest-temperature data have been considered for the fitting since it is known that at higher temperature other modulation mechanisms intervene in addition to the smearing of the Fermi surface.^{2,9} It was also clear at the outset that a strong artificial broadening had to be introduced in the calculation since a rough estimate showed that the experimental structures at very low temperature were at least a factor of 10 broader than what was predicted.¹

Figures 5–7 show, respectively, the comparison between the experimental data of $\Delta R/R$, $\Delta T/T$, and ϵ_2 (the latter with Drude contribution subtracted) with the theoretical line shapes obtained with the following parameters:

$$L_1 - E_F = 3.85 \text{ eV}, \quad (1)$$

$$E_F - L_2' = 0.31 \text{ eV}, \quad (2)$$

$$E_F - L_3 = 3.99 \text{ eV}, \quad (3)$$

$$\frac{|P(d \rightarrow p)|^2}{|P(p \rightarrow s)|^2} = 2.21, \quad (4)$$

where $P(d \rightarrow p)$ and $P(p \rightarrow s)$ are the matrix elements for the $d \rightarrow p$ and $p \rightarrow s$ transitions, respectively. Note that the $L_2'(E_F) \rightarrow L_1$ transitions begin at lower energy than the $L_3 \rightarrow L_2'(E_F)$ transitions, the order being reversed from that previously assigned,^{3,5,11} but in agreement with the order given by Liljenvall and Mathewson.⁴ As Fig. 7 shows, this does not introduce much structure on the rising edge in ϵ_2 . (See also Ref. 4.)

The agreement of theory with experiment for ϵ_2 is very good; the fractional-reflectivity spectra of $\Delta R/R$ also agree fairly well, but the fractional-transmission data $\Delta T/T$ only agree qualitatively. The artificial smearing of the Fermi surface introduced (corresponding to the thermal smearing at 300 K) is necessary to account for both static

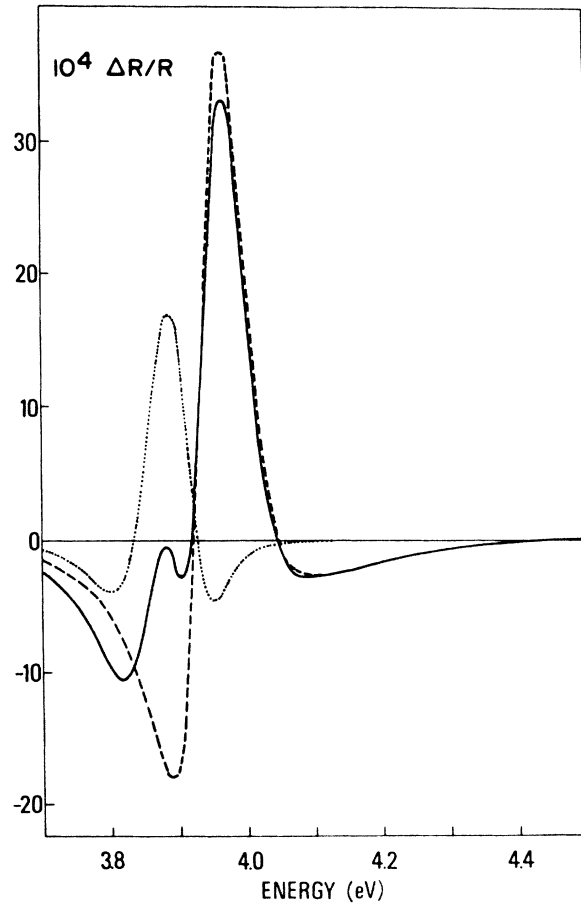


FIG. 8. Theoretical thermoreflection of a 520-Å-thick film of Ag: dotted line; contribution of the $L_2'(E_F) \rightarrow L_1$ transition; dashed line, contribution of the $L_3 \rightarrow L_2'(E_F)$ transition; solid line, total.

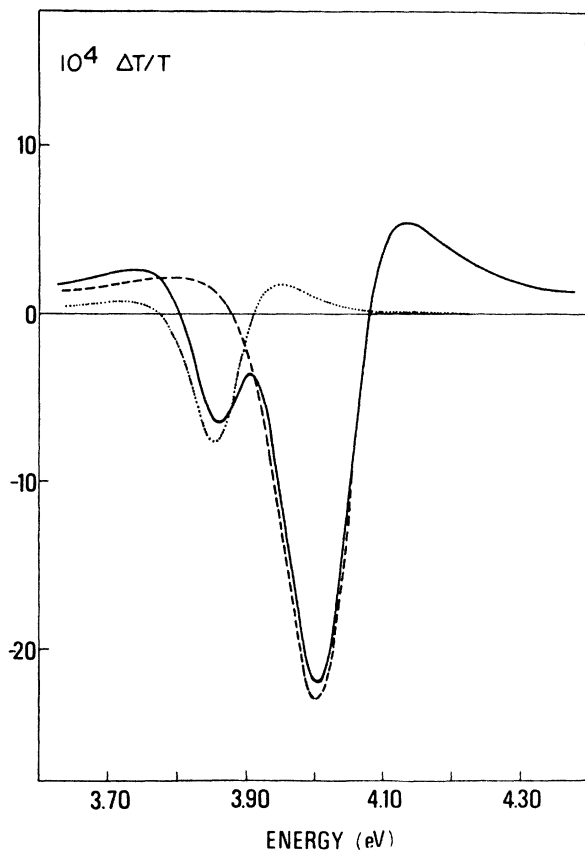


FIG. 9. Theoretical thermotransmission of a 520-Å-thick film of Ag: dotted line, contribution of the $L_2(E_F) \rightarrow L_1$ transition; dashed line, contribution of the $L_3 \rightarrow L_2(E_F)$ transition; solid line, total.

(ϵ_2) and derivative ($\Delta R/R$, $\Delta T/T$) data. This leads to the conclusion that the samples used in these experiments (thin films evaporated on fused-quartz substrates) have a Fermi surface much more smeared out than the actual temperature would account for. The most likely source for this smearing is probably due to the stress produced on the films on cooling from RT to LHeT, due to the difference of thermal expansion coefficients between the sample and quartz substrate. Despite the broadening, these results allow the unequivocal assignment of the contributions of the two different transitions.

Figures 8 and 9 show the theoretical line shapes of $\Delta R/R$ and $\Delta T/T$ divided into their contributions, and Figs. 10 and 11 show the theoretical spectra of $\Delta\epsilon_1$ and $\Delta\epsilon_2$ used to calculate Figs. 8 and 9. The contribution at lower energy has a much smaller magnitude and should therefore be identified as due to the $L_2(E_F) \rightarrow L_1$ transition.

The small peak in $\Delta R/R$ at 3.86 eV (Fig. 3) is seen in the calculated spectrum (Fig. 5) at slightly

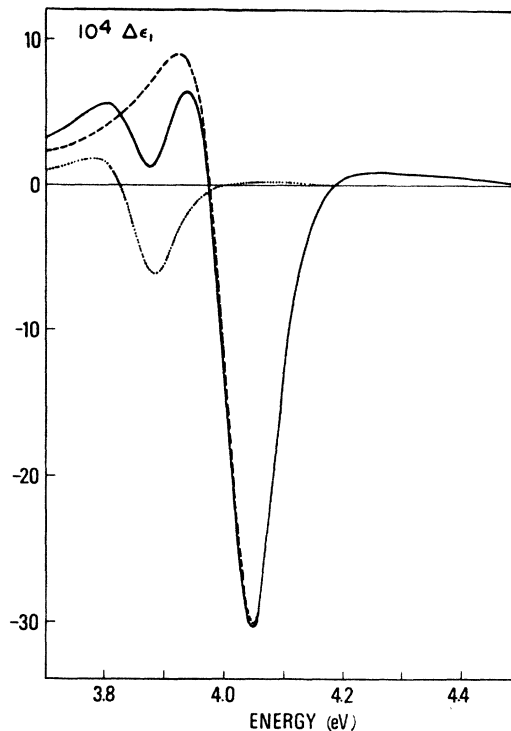


FIG. 10. Theoretical $\Delta\epsilon_1$ of Ag: dotted line, contribution of the $L_2(E_F) \rightarrow L_1$ transition; dashed line, contribution of the $L_3 \rightarrow L_2(E_F)$ transition; solid line, total.

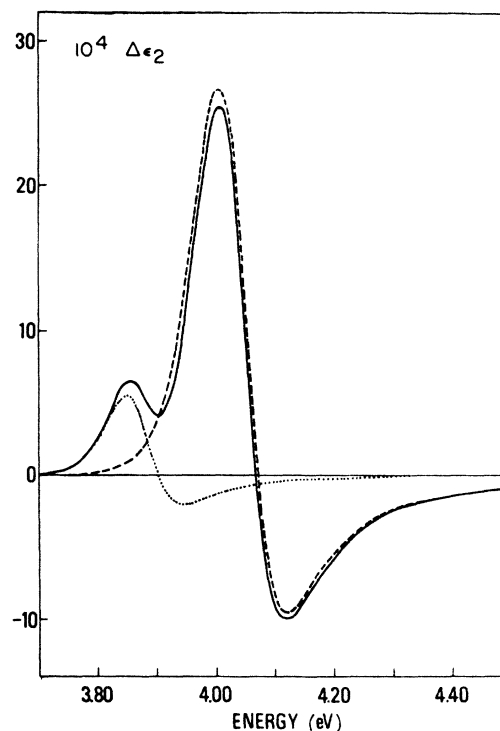


FIG. 11. Theoretical $\Delta\epsilon_2$ of Ag: dotted line, contribution of the $L_2(E_F) \rightarrow L_1$ transition; dashed line, contribution of the $L_3 \rightarrow L_2(E_F)$ transition; solid line, total.

higher energy. Figure 8 shows that it arises from the inter-conduction-band transitions, and, in fact, occurs at the onset of transitions from the Fermi level near L'_2 to the higher conduction band. A similar structure was seen in wavelength-modulation spectra,¹⁸ but at 3.77 eV, which was subsequently attributed to the effect of grain boundaries.¹⁹ We do not believe the 3.77- and 3.86-eV peaks are the same, for the peak at 3.86 eV is readily accounted for by the expected band structure and model for optical transitions.

The peculiarity of thermoderivative spectra of $\Delta\epsilon_1$ and $\Delta\epsilon_2$ taken at low temperature, which arise only from interband transitions involving the Fermi surface, is that they are strictly proportional to the magnitude of the transition.¹ This is certainly an advantage over the piezoderivative technique, where each contribution is weighted with the deformation potential of the bands involved. From the set of calculated parameters we find the value of 4.16 eV for the $L'_2 \rightarrow L_1$ critical point, in very good agreement with previous results.^{7,12} The onsets of the $L'_2(E_F) \rightarrow L_1$ and $L_3 \rightarrow L'_2(E_F)$ transitions occur at 3.87 and 4.03 eV, respectively.

Since the smearing of the Fermi surface affects ϵ_2 only at the onset of the transitions, the good over-all agreement obtained with the experimental ϵ_2 data seem to indicate that the effective masses deduced from Christensen's work⁶ are quite reasonable. The geometrical factors \mathcal{F}_{d-p} and \mathcal{F}_{p-s} introduced in the preceding paper¹ depend only on the effective masses used. Their numerical values

are

$$\mathcal{F}_{d-p} = 0.516, \quad \mathcal{F}_{p-s} = 0.198. \quad (5)$$

Together with the ratio given by Eq. (4), these values yield for the ratio of the magnitudes of the two contributions

$$M^{d-p}/M^{p-s} = 5.76,$$

which should be compared with the value of roughly 4 obtained by Liljenvall and Mathewson⁴ from high-temperature ellipsometric measurements on Ag bulk samples.

IV. CONCLUSIONS

The general features of the theory of thermomodulation of optical transitions involving the Fermi surface in noble metals have been experimentally confirmed. It has been shown that the comparison of very-low-temperature thermomodulation spectra with the theoretical line shape allows the determination of optical band gaps about the Fermi surface with good accuracy.

While thin films deposited on amorphous substrates usually have optical properties very close to bulk samples,²⁰ it has been found that at low temperature a conspicuous broadening takes place probably due to the stress induced on the film by the different coefficients of thermal expansion of the substrate and the film.

ACKNOWLEDGMENT

The authors are grateful to D. W. Lynch for assistance in the preparation of this manuscript.

*Partially supported by an NSF traineeship.

†Present address: Graduate Center for Materials Research, University of Missouri-Rolla, Rolla, Mo. 65401.

¹R. Rosei, preceding paper, Phys. Rev. B **10**, xxx (1974).

²R. Rosei, F. Antonangeli, and U. M. Grassano, Surf. Sci. **37**, 689 (1973).

³C. E. Morris and D. W. Lynch, Phys. Rev. **182**, 719 (1969).

⁴H. G. Liljenvall and A. G. Mathewson, J. Phys. C Suppl. Met. Phys. **3**, 341 (1970).

⁵B. F. Schmidt and D. W. Lynch, Phys. Rev. B **3**, 4015 (1971).

⁶N. E. Christensen, Phys. Status Solidi B **54**, 551 (1972).

⁷L. Walldén and T. Gustafsson, Phys. Scr. **6**, 73 (1972).

⁸G. Baldini and M. Nobile, Solid State Commun. **8**, 7 (1970).

⁹R. Rosei and D. W. Lynch, Phys. Rev. B **5**, 3883 (1972).

¹⁰See Ref. 9 for details of this calculation. In the Appendix of Ref. 9 there are two typographical errors. The expression for $2\Delta K$ should be multiplied by -1 and the expression for $\Delta\epsilon_2$ should have a plus sign instead of a minus.

¹¹R. M. Morgan and D. W. Lynch, Phys. Rev. **172**, 628 (1968).

¹²P. O. Nilsson, Appl. Opt. **7**, 435 (1968).

¹³M. M. Dujardin and M. L. Thèye, J. Phys. Chem. Solids **32**, 2033 (1971).

¹⁴F. Abéles, *Progress in Optics*, edited by E. Wolf (North-Holland, Amsterdam, 1963), p. 251.

¹⁵To perform these calculations ϵ_1 and ϵ_2 data are needed. The theoretical calculation also gives ϵ_2 , but the calculation of ϵ_1 would be a problem. In order to perform a suitable Kramers-Kronig analysis, the spectrum of ϵ_2 would be needed over a infinite range of energy. Instead the approximation upon which the calculation is based is valid only a few tenths of an eV above the onset of the transitions. Therefore, experimental data (from Ref. 11) have been chosen for ϵ_1 and ϵ_2 .

¹⁶D. Shoenberg, Philos. Trans. R. Soc. Lond. A **255**, 85 (1962).

¹⁷C. N. Berglund and W. E. Spicer, Phys. Rev. **136**, A1044 (1964).

¹⁸M. Welkowsky and R. Braunstein, Solid State Commun. **9**, 2139 (1971).

¹⁹O. Hunderi, Phys. Rev. B **7**, 3419 (1973).

²⁰M. L. Thèye, Phys. Rev. B **2**, 3060 (1970).